

Epitaxial orientation of Mg₂Si(110) thin film on Si(111) substrate

Y. Wang

*Beijing National Laboratory for Condensed Matter Physics, Institute of Physics, Chinese Academy of Sciences, Beijing 100080, China and School of Engineering, The University of Queensland, St. Lucia QLD 4072, Australia*X. N. Wang, Z. X. Mei, and X. L. Du^{a),b)}*Beijing National Laboratory for Condensed Matter Physics, Institute of Physics, Chinese Academy of Sciences, Beijing 100080, China*J. Zou^{a),c)}*School of Engineering, The University of Queensland, St. Lucia QLD 4072, Australia and Centre for Microscopy and Microanalysis, The University of Queensland, St. Lucia QLD 4072, Australia*

J. F. Jia and Q. K. Xue

Department of Physics, Tsinghua University, Beijing 100084, China and Institute of Physics, Chinese Academy of Sciences, Beijing 100080, China

X. N. Zhang and Z. Zhang

Beijing University of Technology, Beijing 100022, China

(Received 16 June 2007; accepted 23 October 2007; published online 19 December 2007)

Epitaxial Mg₂Si(110) thin film has been obtained on Si(111) substrate by thermally enhanced solid-phase reaction of epitaxial Mg film with underlying Si substrate. An epitaxial orientation relationship of Si(111)∥Mg₂Si(110) and Si(1 $\bar{1}$ 0)∥Mg₂Si(1 $\bar{1}$ 0) has been revealed by transmission electron microscopy. The formation of the unusual epitaxial orientation relationship is attributed to the strain relaxation of Mg₂Si film in a MgO/Mg₂Si/Si double heterostructure. © 2007 American Institute of Physics. [DOI: 10.1063/1.2821916]

Mg₂Si has promising applications in the infrared optoelectronic devices.¹ Many attempts have been made to prepare Mg₂Si films on Si substrates due to their potential applications.^{2–4} However, the fact that Mg has a low condensation coefficient with Si and a high vapor pressure even at 200 °C (~10⁻⁷ mbar) makes it a formidable task to grow Mg₂Si epitaxial films on Si substrates.^{1,5} In addition, the lattice mismatch between fcc Mg₂Si (*a*=0.635 nm) and Si (*a*=0.539 nm) is as large as 18%. As a consequence, no single-crystalline Mg₂Si thin film with a thickness over 1 nm has been satisfactorily achieved so far, although many efforts have been devoted to improve the growth methods.^{1,6–8} Brause *et al.*⁶ acquired a Mg₂Si layer on (111) Si without an epitaxial relationship between them. Hosono *et al.*⁷ obtained polycrystalline Mg₂Si with predominant (211) texture by heating a bulk (111) Si under Mg vapor. By using molecular beam epitaxy (MBE), Mahan *et al.*¹ achieved a polycrystalline Mg₂Si thin film with (111) texture on both (111) and (100) Si substrates by codeposition of Mg with Si at 200 °C, and they found no accumulation of Mg or formation of Mg silicide on Si after reactive deposition of Mg onto the Si substrate at 200 °C. It has been reported by several researchers that Mg₂Si(111) layer would form on Si(111) surface during the Mg deposition on Si(111).^{8–10} In their reports, it was found that, to minimize the *in-plane* lattice mismatch between Mg₂Si(111) and Si(111) planes, there was a 30°

rotation between Mg₂Si(111) and Si(111) planes along the [111] direction. However, the grown Mg₂Si layer can only be very thin (≤0.6 nm), otherwise, the Mg₂Si layer would be covered by metal Mg as Mg vapor continues. Until now, no uniform Mg₂Si thin film has been achieved on Si. In this study, we demonstrate the realization of an epitaxial Mg₂Si(110) film on Si(111) in a MBE system. An unusual epitaxial relationship has been revealed. By using several techniques of transmission electron microscopy (TEM), the film formation mechanism has been investigated by focusing on the capping layer induced compressive strain in the Mg₂Si film.

The Mg₂Si thin films studied here were prepared by using the thermally enhanced solid-phase reaction of epitaxial Mg film with underlying Si(111) substrate in a radio frequency plasma-assisted MBE system (OmniVac).¹¹ Before being loaded into the growth chamber, the Si wafers were degreased in acetone and trichloroethylene, then etched with 5% HF solution for 5 min and rinsed in de-ionized water. A Mg film with a nominal thickness of ~6 nm was deposited on Si(111) with a rate of 0.2 Å/s under ultrahigh vacuum condition at -20 °C. Considering the high vapor pressure of Mg, a capping layer involving 4 nm thick MgO and 100 nm thick ZnO films was prepared on Mg layer to prevent Mg from reevaporation during the temperature ramping and annealing. After that, the sample was heated to 100 °C to enhance the solid-phase reaction between Mg and Si. Finally, an epitaxial Mg₂Si film was obtained after 3 h annealing at this temperature. The samples were investigated by cross-sectional TEM in a Philips CM200 field emission gun TEM

^{a)}Authors to whom correspondence should be addressed.^{b)}Electronic mail: xldu@aphy.iphy.ac.cn.^{c)}Electronic mail: j.zou@uq.edu.au.

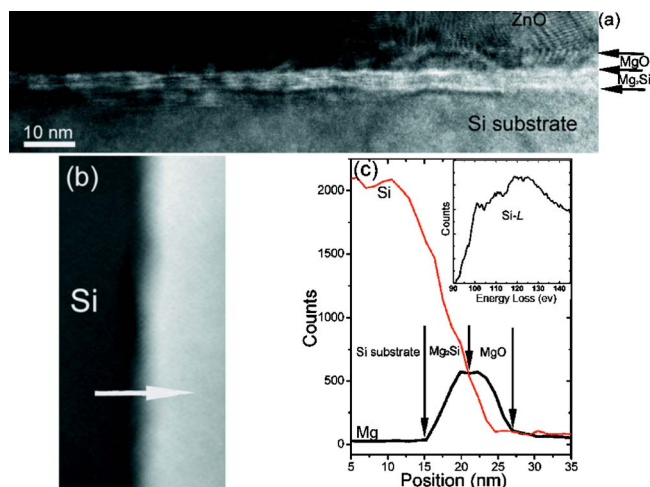


FIG. 1. (Color online) (a) A bright-field TEM image showing a uniform layer above the Si substrate. (b) A dark-field STEM image and (c) elemental profiles extracted from (b) showing distribution of elements (Si and Mg) within the film. The inset in (c) is the Si *L* edge of the EELS profile.

equipped with a Gatan image filtering system and a Tecnai F20 field emission gun TEM [equipped with a scanning functionality (STEM) and an energy dispersive spectroscopy (EDS)]. TEM specimens were prepared by the conventional mechanical grinding and polishing, followed by the ion beam thinning in a Gatan precision ion polisher system.

Figure 1(a) is a low magnification bright-field TEM image and shows the typical overview of the thin film with respect to the Si substrate. As indicated in the figure, a white thin layer with uniform thickness sandwiched between the Si substrate and the MgO topmost layer is clearly illustrated, and the MgO layer shows an island character. To understand the chemical component of these layers, STEM/EDS analyses were carried out and the results are shown in Figs. 1(b) and 1(c), respectively. Figure 1(b) is a dark-field STEM image in the area containing all epitaxial layers and the Si substrate. Figure 1(c) shows the EDS line-scan profiles of Si and Mg, respectively, along the growth direction [as indicated in Fig. 1(b)]. These profiles qualitatively demonstrate the variations of both elements across different layers, from which one can conclude that the layer adjacent to the Si substrate contains both Mg and Si. There is only one stoichiometric magnesium silicide phase, i.e., Mg₂Si, available in the Si-Mg phase diagram.⁶ Besides, our EDS point analysis for this layer suggests a Mg/Si ratio of 2. This result was also confirmed by the electron energy loss spectroscopy (EELS) results [the inset of Fig. 1(c)], in which the Si *L* edge is similar to the Si *L* edge found in bulk Mg₂Si.¹² Therefore, we anticipate that this layer is Mg₂Si.

To understand the interface structure between Mg₂Si and Si at atomic level, high resolution TEM (HRTEM) was carried out. Figures 2(a) and 2(b) are typical HRTEM images taken along Si [1 $\bar{1}0$] and [11 $\bar{2}$] directions (both perpendicular to each other), respectively. A very sharp Mg₂Si/Si interface is observed, indicating a well-defined epitaxial layer of Mg₂Si with a thickness of ~ 3.5 nm, which is consistent with the observation on Fig. 1(a), where the thickness of the Mg₂Si layer is very uniform.

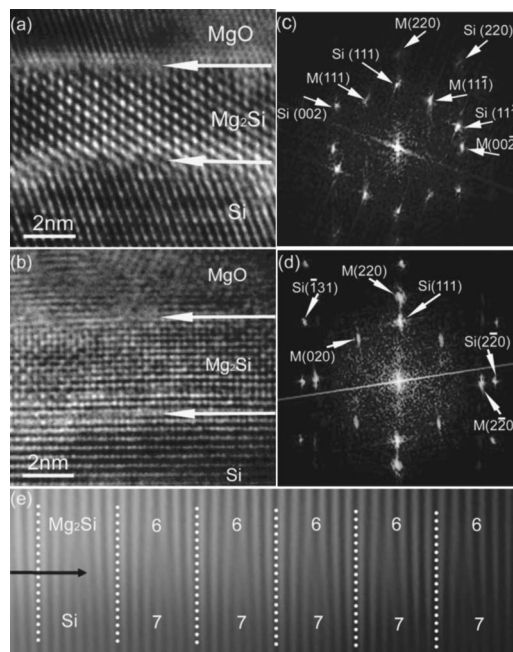


FIG. 2. Typical HRTEM images along (a) Si[1 $\bar{1}0$] and (b) Si[11 $\bar{2}$], respectively, showing atomic structures of the Mg₂Si thin film and its associated interfaces. [(c) and (d)] Fast Fourier transformations taken respectively from (a) and (b) in which the regions contain the Mg₂Si/Si interfaces. The diffraction spots indexed with M denote Mg₂Si. (e) A Fourier-filtered HREM image from (b) using diffraction spots Si(2 $\bar{2}0$) and Mg₂Si(2 $\bar{2}0$), showing every six Mg₂Si(2 $\bar{2}0$) planes match well with seven Si(2 $\bar{2}0$) planes (counted from the dotted lines).

To determine the epitaxial relationship between the Mg₂Si thin film and its underlying Si substrate, fast Fourier transformations (FFTs) (equivalent to the electron diffraction) were taken from the Mg₂Si/Si interfacial region of the HRTEM images as shown in Figs. 2(a) and 2(b),¹³ and results are shown in Figs. 2(c) and 2(d), respectively. By careful indexing the two FFT patterns (as indicated in the FFT patterns, where *M* denotes Mg₂Si), the crystallographic orientation relationship between Mg₂Si and Si can be determined as Si[111]||Mg₂Si[110], Si[1 $\bar{1}0$]||Mg₂Si[1 $\bar{1}0$], and Si[11 $\bar{2}$]||Mg₂Si[00 $\bar{1}$].

To understand the nature of such an in-plane epitaxial relationship, we examined the equilibrium lattice mismatches $F_{Si\{hkl\}||Mg_2Si\{h'k'l'\}} = (D_{Mg_2Si\{h'k'l'\}} - D_{Si\{hkl\}}) / D_{Si\{hkl\}}$, where $D_{A\{hkl\}}$ is the lattice spacing of the {*hkl*} atomic planes for material *A* in the two perpendicular in-plane directions. A schematic diagram of in-plane atomic structure [the Mg₂Si(110) atomic plane superimposed with the Si(111) atomic plane] is shown in Fig. 3. Based on their lattice parameters, $F_{3\times Si\{2\bar{2}4\}||Mg_2Si\{00\bar{2}\}} = -3.8\%$ and $F_{Si\{2\bar{2}0\}||Mg_2Si\{2\bar{2}0\}} = 17.8\%$, in which the positive sign means that the epitaxial layer experienced a compressive stress and the negative sign indicates a tensile stress applied on the epitaxial layer. As can be expected, such lattice mismatches can generate significant misfit strains in different directions, particularly for the [1 $\bar{1}0$] direction, in which the lattice mismatch reaches 17.8%. To understand how this huge lattice mismatch was accommodated between Mg₂Si and Si, its interfacial structure was investigated. To do this, Fourier-filtered TEM image of the

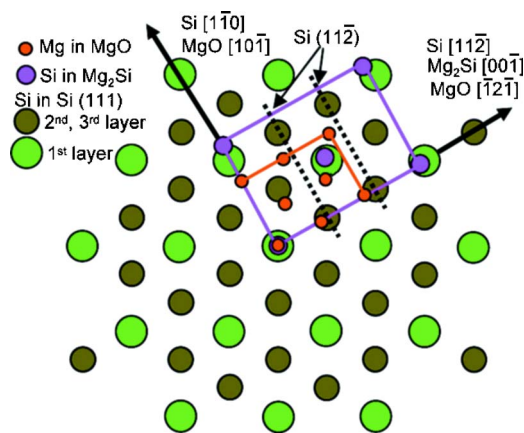


FIG. 3. (Color online) A schematic diagram showing the atomic arrangement of MgO(111)/Mg₂Si(110) planes on Si(111) plane, where Si[1 $\bar{1}0$] \parallel Mg₂Si[1 $\bar{1}0$] \parallel MgO[10 $\bar{1}$] and Si[11 $\bar{2}$] \parallel Mg₂Si[00 $\bar{1}$] \parallel MgO[1 $\bar{2}$ $\bar{1}$].

interfacial region¹⁴ was acquired from Fig. 2(b) and the result is shown in Fig. 2(e). As can be clearly seen, for every seven Si{2 $\bar{2}0$ } atomic planes, there were six Mg₂Si atomic planes to associate them (indicated by dotted lines), and such domain match periodically appeared. Based on the theoretical lattice parameters of Si and Mg₂Si, the $7 \times \{2\bar{2}0\}_{\text{Si}} : 6 \times \{2\bar{2}0\}_{\text{Mg}_2\text{Si}}$ match can relieve a misfit strain of 16.8%, leaving a residual misfit strain (compressive) of 1% (17.8%–16.8%) in that direction. By such a $7 \times \{2\bar{2}0\}_{\text{Si}} : 6 \times \{2\bar{2}0\}_{\text{Mg}_2\text{Si}}$ match, we have misfit strains (f) of $f=1\%$ in the $[1\bar{1}0]_{\text{Si}}$ direction and $f=-3.8\%$ in the $[1\bar{1}2]_{\text{Si}}$ direction.

The question now is why and how the cubic Mg₂Si layer form in such an epitaxial relationship, but not as reported previously,^{9,10} with Si during the annealing. To answer this question, we note that a MgO(111)/Mg(0001)/Si(111) double heterostructure was formed at low temperature.¹¹ The annealing of this structure at 100 °C greatly enhanced the solid-phase reaction of the Mg film with the Si substrate due to the reactive nature of the Mg/Si interface even at room temperature, resulting in the formation of cubic Mg₂Si,^{8,9} i.e., MgO(111)/Mg₂Si/Si(111) structure was formed under this thermoequilibrium condition. It is anticipated that such a reaction drives the entire system toward to the stable situation (lower the system energy). To confirm this, we compare the misfit strains of the system before and after the annealing process. It has been reported¹¹ that the as-grown structure contains the Si substrate with the Mg layer and MgO layer on top of Si and they have an in-plane epitaxial relationship of $\langle 11\bar{2} \rangle_{\text{Si}} \parallel \langle 10\bar{1}0 \rangle_{\text{Mg}} \parallel \langle 11\bar{2} \rangle_{\text{MgO}}$. Based on their lattice parameters, the lattice mismatches between Si and Mg can be estimated respectively as 26% in the $[11\bar{2}]_{\text{Si}}$ direction and –16% in the $[1\bar{1}0]_{\text{Si}}$ direction. As discussed above, the misfit strains between Mg₂Si and Si are –3.8% in the $[11\bar{2}]_{\text{Si}}$ direction and 1% in the $[1\bar{1}0]_{\text{Si}}$ direction (as most of the misfit strain in this direction has been relieved through the formation of regular misfit dislocations during the Mg₂Si formation), which is significantly lower than the Mg/Si case. In addition, the signs of in-plane misfit strains are opposite, i.e., compressive in one direction and tensile in the orthogonal

direction, so that most of the in-plane misfit strains can be compensated within the interface by the in-plane distortion. In contrast, for the reported epitaxial relationship $\{111\}_{\text{Si}} \parallel \{111\}_{\text{Mg}_2\text{Si}}$ and $\langle 110 \rangle_{\text{Si}} \parallel \langle 112 \rangle_{\text{Mg}_2\text{Si}}$,^{8,9} although the theoretical lattice mismatch is only $\sim 2\%$, the Mg₂Si layer, in fact, experiences a compressive stress from all directions within the interface, which must be more significant than our case. This analysis suggests that our epitaxial relationship must be energetically favorable.

It is of interest to explore the role of MgO upon the formation of such an epitaxial relationship. Since the Mg₂Si layer is formed by the solid-phase reaction between Mg and Si, where MgO is a capping layer that prevents the desorption of Mg atoms during the annealing treatment and ensures the formation of such a uniform Mg₂Si layer. Interestingly, the MgO layer tends to have an epitaxial relationship with the underlying Mg₂Si, with MgO (111)_{MgO} \parallel (110)_{Mg₂Si} and MgO $[10\bar{1}]_{\text{MgO}} \parallel [1\bar{1}0]_{\text{Mg}_2\text{Si}}$. Although the theoretical lattice mismatches in such an epitaxial relationship can be estimated respectively as $\sim 7\%$ in the $\langle 1\bar{2}\bar{1} \rangle_{\text{MgO}}$ direction and –34% in the $\langle 1\bar{1}0 \rangle_{\text{MgO}}$ direction, the fact that the MgO layer has a structural characteristic of islands suggests that the MgO layer can tolerate (e.g., relax) more distortion or a large amount of lattice mismatches induced during the reaction than the underlying Si substrate does. In addition, the ZnO overlayer should also play a similar role as the MgO on the formation of the Mg₂Si layer during the annealing.

In conclusion, single-crystalline Mg₂Si thin films have been achieved on (111) Si by the thermally enhanced solid-phase reaction of epitaxial Mg overlayer with Si substrate in a MBE system. An unusual epitaxial relationship between Si and Mg₂Si has been identified with Si(111) \parallel Mg₂Si(110) and Si[1 $\bar{1}0$] \parallel Mg₂Si[1 $\bar{1}0$].

The National Science Foundation of China (50532090, 60476044, 60606023, and 10604007), the Ministry of Science and Technology of China (2002CB613502), Chinese Academy of Sciences, and the Australia Research Council (DP0663304) are acknowledged for their financial support.

¹J. E. Mahan, A. Vantomme, G. Langouche, and J. P. Becker, Phys. Rev. B **54**, 16965 (1996).

²P. L. Janega, J. McCaffrey, D. Landheer, M. Buchanan, M. Denhoff, and D. Mitchell, Appl. Phys. Lett. **53**, 2056 (1988).

³M. Akiya and H. Nakamura, J. Appl. Phys. **59**, 1596 (1986).

⁴H. N. Zhu, K. Y. Gao, and B. X. Liu, Phys. Rev. B **62**, 1647 (2000).

⁵A. Vantomme, J. E. Mahan, G. Langouche, J. P. Becker, M. V. Bael, K. Temst, and C. V. Haesendonck, Appl. Phys. Lett. **70**, 1086 (1997).

⁶M. Brause, B. Braun, D. Ochs, W. Maus-Friedrichs, and V. Kempter, Surf. Sci. **398**, 184 (1998).

⁷T. Hosono, Y. Matsuzawa, M. Kuramoto, Y. Momose, H. Tatsuoka, and H. Kuwabara, Solid State Phenom. **93**, 447 (2003).

⁸J. Quinn and F. Jona, Surf. Sci. **249**, L307 (1991).

⁹C. Wigren, J. N. Andersen, R. Nyholm, and U. O. Karlsson, Surf. Sci. **289**, 290 (1993).

¹⁰K. S. An, R. J. Kim, C. Y. Park, S. B. Lee, T. Abukawa, S. Kono, T. Kinoshita, A. Kakizaki, and T. Ishii, J. Appl. Phys. **78**, 1151 (1995).

¹¹X. N. Wang, Y. Wang, Z. X. Mei, J. Dong, Z. Q. Zeng, H. T. Yuan, T. C. Zhang, X. L. Du, J. F. Jia, Q. K. Xue, X. N. Zhang, Z. Zhang, Z. F. Li, and W. Lu, Appl. Phys. Lett. **90**, 151912 (2007).

¹²S. Miao, Ph.D. thesis, California Institute of Technology, 2007.

¹³Y. Wang, X. L. Du, Z. X. Mei, Z. Q. Zeng, M. J. Ying, H. T. Yuan, J. F. Jia, Q. K. Xue, and Z. Zhang, Appl. Phys. Lett. **87**, 051901 (2005).

¹⁴J. Narayan and B. C. Larson, J. Appl. Phys. **93**, 278 (2003).